Gene-Targeted Next Generation Sequencing Identifies *PNPLA1* Mutations in Patients with a Phenotypic Spectrum of Autosomal Recessive Congenital Ichthyosis: The Impact of Consanguinity

Hassan Vahidnezhad[1,2,14], Leila Youssefian[1,3,14], Amir Hossein Saeidian[1], Sirous Zeinali[2,4], Parvin Mansouri[5], Soheila Sotoudeh[6], Mohammadreza Barzegar[7], Javad Mohammadi-asl[8], Razieh Karamzadeh[9,10], Maryam Abiri[3], Kevin McCormick[11], Paolo Fortina[11,12] and Jouni Uitto[1,13]

Autosomal recessive congenital ichthyosis is a heterogeneous group of disorders associated with mutations in at least nine distinct genes. To ascertain the molecular basis of ichthyosis patients in Iran, a country of approximately 80 million people with a high prevalence of customary consanguineous marriages, we have developed a gene-targeted next generation sequencing array consisting of 38 genes reported in association with ichthyosis phenotypes. In a subset of nine extended consanguineous families, we found homozygous missense mutations in the *PNPLA1* gene, six of them being distinct and, to our knowledge, previously unpublished. This gene encodes an enzyme with lipid hydrolase activity, important for development and maintenance of the barrier function of the epidermis. These six mutations, as well as four previously published mutations, reside exclusively within the patatin-like subdomain of *PNPLA1* containing the catalytic site. The mutations clustered around the active center of the enzyme or resided at the surface of the protein possibly involved in the protein-protein interactions. Clinical features of the patients showed considerable intra- and interfamilial heterogeneity. Knowledge of the specific mutations allows identification of heterozygous carriers, assisting in genetic counseling, prenatal testing, and preimplantation genetic diagnosis in extended families at risk of recurrence of this disorder, the incidence of which is significantly increased in consanguineous marriages.

Journal of Investigative Dermatology (2017) **137,** 678–685; doi:10.1016/j.jid.2016.11.012

[1]*Department of Dermatology and Cutaneous Biology, Sidney Kimmel Medical College, Thomas Jefferson University, Philadelphia, Pennsylvania, USA;* [2]*Biotechnology Research Center, Department of Molecular Medicine, Pasteur Institute of Iran, Tehran, Iran;* [3]*Department of Medical Genetics, Tehran University of Medical Sciences, Tehran, Iran;* [4]*Kawsar Human Genetics Research Center, Tehran, Iran;* [5]*Skin and Stem Cell Research Center, Tehran University of Medical Sciences, Tehran, Iran;* [6]*Department of Dermatology, Children's Medical Center, Center of Excellence, Tehran University of Medical Sciences, Tehran, Iran;* [7]*Skin Research Center, Shahid Beheshti University of Medical Sciences, Tehran, Iran;* [8]*Department of Genetics, Ahvaz Jundishapur University of Medical Sciences, Ahvaz, Iran;* [9]*Institute of Biochemistry and Biophysics, University of Tehran, Tehran, Iran;* [10]*Department of Molecular Systems Biology, Cell Sciences Research Center, Royan Institute for Stem Cell Biology and Technology, ACECR, Tehran, Iran;* [11]*Sidney Kimmel Cancer Center, Department of Cancer Biology, Thomas Jefferson University, Philadelphia, Pennsylvania, USA;* [12]*Department of Molecular Medicine, Sapienza University, Rome, Italy; and* [13]*Jefferson Institute of Molecular Medicine, Thomas Jefferson University, Philadelphia, Pennsylvania, USA*

[14]*These authors contributed equally to this work.*

Correspondence: Jouni Uitto, Department of Dermatology and Cutaneous Biology, Sidney Kimmel Medical College at Thomas Jefferson University, 233 South 10th Street, Suite 450 BLSB, Philadelphia, PA 19107, USA. E-mail: Jouni.Uitto@jefferson.edu

Abbreviations: ARCI, autosomal recessive congenital ichthyosis; bp, base pair; NGS, next generation sequencing

Received 1 September 2016; revised 25 October 2016; accepted 7 November 2016; accepted manuscript published online 21 November 2016; corrected proof published online 21 November 2016

INTRODUCTION

Heritable forms of ichthyoses, also referred to as generalized Mendelian disorders of cornification, are phenotypically a highly heterogeneous group of conditions caused by mutations in a number of genes playing a role in keratinocyte differentiation and epidermal barrier function (Baden and Digiovanna, 2013; Schmuth et al., 2013). These diseases are characterized by scaling and hyperkeratosis with associated cutaneous and extracutaneous features. This group of disorders is also genetically heterogeneous, with autosomal dominant, autosomal recessive, and X-linked inheritance being described. A specific subgroup of inherited ichthyoses is the autosomal recessive congenital ichthyosis (ARCI), with many newborns presenting as collodion babies, but the subsequent clinical presentation and the spectrum of severity can be highly variable (Richard and Bale, 2014). In the most severe forms, such as harlequin ichthyosis, the disease is often fatal during the early postnatal period, whereas at the other end of the continuum of the spectrum, the disease may present with a relatively mild scaling and variable degree of palmoplantar keratoderma. There is considerable genetic heterogeneity in ARCI, and as many as nine different genes are known to harbor biallelic mutations; these include *TGM1*, *ALOXE3*, *ALOX12B*, *NIPAL4*, *ABCA12*, *CYP4F22*, *PNPLA1*, *LIPN*, and *CERS3*. Previous reports have suggested that mutations in *TGM1* account for 30–65% of all

patients with ARCI, whereas mutations in *LIPN*, *PNPLA1*, and *CERS3* have been reported only in a few consanguineous families (Richard and Bale, 2014).

With the advent of next generation sequencing (NGS), there has been tremendous progress in facilitating the mutation detection in various heritable skin disorders, including ichthyosis (South et al., 2015; Takeichi et al., 2013). In fact, at least 38 different genes have now been suggested to be associated with the ichthyotic phenotypes, either as the primary mutated genes or modifying the phenotypic presentation. To elucidate the genetic basis of ichthyosis in Iran, a country of approximately 80 million people with high prevalence of customary consanguineous marriages, we developed a gene-targeted NGS array consisting of 38 genes reported in association with ichthyosis phenotypes. Identification of specific mutations in a large number of families has allowed us to examine phenotype/genotype correlations with respect to both intra- and interfamilial heterogeneity, in part because of extensive consanguinity in these families. In this study, we identified six distinct and, to our knowledge, previously unreported mutations in the *PNPLA1* gene in nine families.

RESULTS

Mutation detection in *PNPLA1*

In attempts to decipher the underlying molecular basis in patients diagnosed with different forms of ichthyosis, we first developed a gene-targeted NGS array that covered all coding exons, at least 20 base pairs (bp) of the flanking intronic sequences, and up to 50 bp of 3′-untranslated regions of 38 genes known to be associated with various forms of ichthyosis. The amplicon panel was designed to cover 99% of the targeted bases, and NGS sequencing metadata indicated that 98.0% and 95.5% of these bases had a minimum coverage of 10× and 30×, respectively. The minimum coverage for *PNPLA1* was 188×, and the maximum coverage was 1,509×, with a mean of 1,055×. (For details of sample preparation, library construction, mutation detection, and bioinformatics analysis of the data, see Materials and Methods).

Among the total of 92 probands, each representing a distinct extended family, with clinical diagnosis of a nonsyndromic or syndromic form of ichthyosis (Figure 1), a subgroup of patients representing nine families was found to have homozygous, potentially pathogenic mutations in the *PNPLA1* gene, all of the mutations being previously unreported to our knowledge (Table 1, Supplementary Table S1 online, and Figure 2). The presence of these sequence variants in genomic DNA was confirmed by bidirectional Sanger sequencing. All the sequence variants were missense mutations, and bioinformatics analysis by mutation prediction programs, including PolyPhen2, FIS, GVGD, PROVEAN, and SIFT, predicted these mutations to be pathogenic (Table 1). Furthermore, these sequence variants were absent in 119,654 alleles in the control population, with the exception of the p.Asp172Asn substitution, which was reported heterozygous in one allele (ExAC.broadinstitute.org), although our patients were homozygous for this mutation. The segregation of these mutations with the phenotype was confirmed by genotyping all available family members, which showed homozygous mutations in all affected individuals tested and that the tested parents were heterozygous carriers. The patients and parents tested for the mutations in families 1–9 are indicated in Figure 2.

In two families of no known relationship (families 1 and 2), the same mutation, c.56C>T, p.Ser19Leu, was noted. In two other apparently unrelated families (families 8 and 9), the same mutation, c.514G>A, p.Asp172Asn, was present, and in another two unrelated families (families 5 and 6), a c.421A>G, p.Lys141Glu mutation was present (Figure 2). We subsequently examined the possibilities that these mutations are either results of a founder effect or are hotspot mutations. Haplotype analysis with four intragenic single-nucleotide polymorphisms (SNPs), which were disclosed during sequencing of the gene, was performed for all six patients with these mutations. The results showed two conserved homozygosity blocks within the genomic region harboring *PNPLA1* with these mutations, suggesting a founder effect in these Iranian patients of different ethnicity and language groups. Specifically, families 1 and 2, both of Persian ethnicity and with the p.Ser19Leu mutation, had the same haplotype comprising four intragenic SNPs, including a very rare SNP, rs34598813, within the exon 6 of *PNPLA1* (minor allele frequency: 0.08 [G]). Families 5 and 6, who had the p.Lys141Glu mutation and were from Kurdish and Persian backgrounds, respectively, and Families 8 and 9, who had the p.Asp172Asn mutation, had the same unique haplotype, but it was different from the p.Ser19Leu-related haplotype.

Of particular interest was the mutation c.100G>C, p.Ala34Pro in Family 3, previously unreported to our knowledge. This same Ala34 residue was previously shown to be mutated to threonine (p.Ala34Thr) (Fachal et al., 2014). These observations provided evidence for the critical importance of the Ala34 residue in the function of PNPLA1.

The gene-targeted sequencing panel also identified a heterozygous sequence variant, c.1464T>A, p.Tyr488Ter, in two unrelated families, raising the possibility that these patients might be compound heterozygous for *PNPLA1* mutations. However, one of these families with the ARCI phenotype was subsequently shown to harbor a homozygous sequence variant in another gene, *ST14*, previously reported in a syndromic form of ichthyosis (Alef et al., 2009; Basel-Vanagaite et al., 2007), suggesting that the heterozygous premature termination codon causing sequence variant in *PNPLA1* was coincidental and unlikely to be pathogenic. In all probands with homozygous *PNPLA1* mutations, heterozygous sequence variants in 37 other ichthyosis-associated genes were also identified (see Supplementary Table S2 online). In particular, eight of the nine probands had a heterozygous *NIPAL4* variant, p.Glu64Lys, which was absent from 60,706 unrelated control individuals in ExAC Browser (exac.broadinstitute.org). However, this variant (NIPAL4: NM_001099287) was found to be frequent in Iranian individuals without ichthyosis, present in 84 out of 184 independent alleles (45.6%), indicating that p.Glu64Lys is a common polymorphism in this population. Considering the consanguinity in these individuals with homozygous *PNPLA1* mutations, the heterozygous variants are unlikely to be of pathological significance. However, in family 3, two allelic variants, p.Glu64Lys and p.Val244Phe, were disclosed in the *NIPAL4* gene, previously shown to harbor mutations in ARCI6. Although these mutations may be pathogenic or may

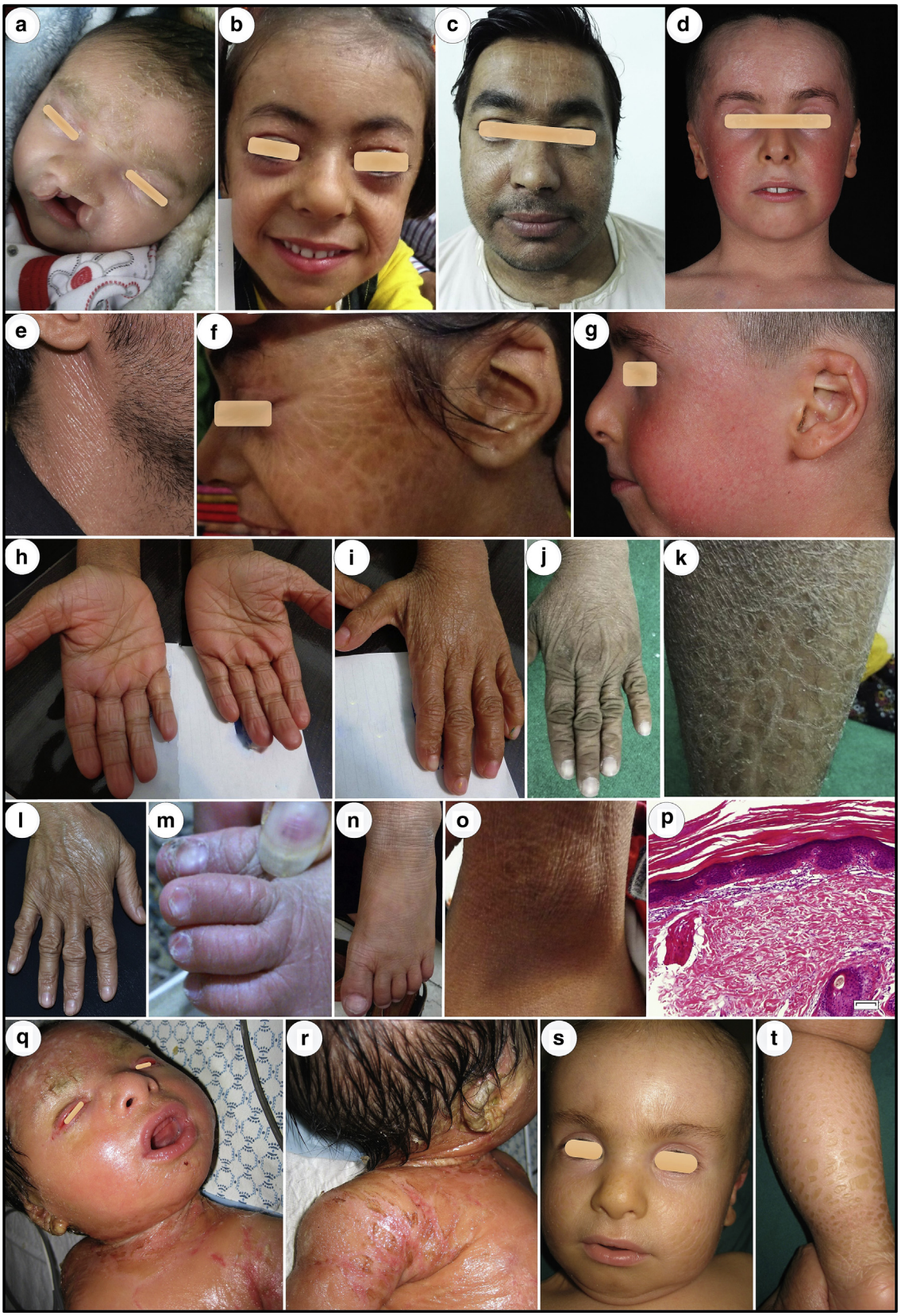

Figure 1. Clinical features and histopathology of patients with *PNPLA1* mutations. (**a**–**f, k, o**) Note hyperkeratotic scaly lesions with ectropion, as well as (**h**) hyperlinearity of the palms, and (**i, j**) acrogeric features on the backs of the hands in a 7-year-old patient, and (**l**) of a 32-year old patient. Also note (**d, g**) erythroderma, (**f, g**) malformation of the outer ears, and (**m, n**) nail dystrophy. (**p**) Characteristic histopathological findings include lamellar orthokeratosis, focal parakeratosis, and mild psoriasiform acanthosis; granular layer appears normal in epidermis. In the upper dermis, there is vascular proliferation, ectasia, and sparse perivascular inflammatory cell infiltrate. Scale bar = 50 μm). (**q**–**t**) Illustration of the evolvement of the clinical phenotype of the 8-year-old patient shown in **d** and **g**, showing (**q, r**) collodion membrane at birth, (**s, t**) which resolved 1 year later. All subjects and parents of underaged patients gave written informed consent to publish their images.

Table 1. *PNPLA1*-associated autosomal recessive congenital ichthyosis with previously unreported pathogenic mutations

Family Number	Number of Patients in Family	Age of Patients, years	Consanguinity of Proband's Parents	Ethnicity	Mutation at cDNA Level	Mutation at Protein Level	Exon	PolyPhen2 Score[1]	FIS of Mutation Assessor[2]	GD Score of Align GVGD[3]	Score of PROVEAN (Cutoff = −2.5)[4]	SIFT[5]
1	1	4	First cousin	Persian	c.56C>T	p.S19L	1	1 (Probably damaging)	3.225 (Medium)	144.08 (Class C65)	−3.284 (Deleterious)	0 (Damaging)
2	3	20–29	First cousin once removed	Persian	c.56C>T	p.S19L	1	1 (Probably damaging)	3.225 (Medium)	144.08 (Class C65)	−3.284 (Deleterious)	0 (Damaging)
3	3	25–36	First cousin	Lurish	c.100G>C	p.A34P	1	1 (Probably damaging)	2.860 (Medium)	26.87 (Class C25)	−3.229 (Deleterious)	0.01 (Damaging)
4	1	37	First cousin	Persian	c.374C>A	p.T125N	2	1 (Probably damaging)	3.005 (Medium)	64.77 (Class C55)	−4.829 (Deleterious)	0 (Damaging)
5	4	3–23	First cousin	Kurdish	c.421A>G	p.K141E	2	0.982 (Probably damaging)	2.600 (Medium)	56.87 (Class C55)	−3.644 (Deleterious)	0.02 (Damaging)
6	5	15–33	Second cousin	Persian	c.421A>G	p.K141E	2	0.982 (Probably damaging)	2.600 (Medium)	56.87 (Class C55)	−3.644 (Deleterious)	0.02 (Damaging)
7	6	7–24	First cousin	Arab	c.488C>T	p.P163L	3	1 (Probably damaging)	2.335 (Medium)	97.78 (Class C65)	−10.000, (Deleterious)	0.07 (Tolerated)
8	1	7	First cousin	Lurish	c.514G>A	p.D172N	4	1 (Probably damaging)	3.360 (Medium)	97.78 (Class C65)	−4.995 (Deleterious)	0 (Damaging)
9	2	17–33	First cousin	Azeri	c.514G>A	p.D172N	4	1 (Probably damaging)	3.360 (Medium)	23.01 (Class C15)	-4.995 (Deleterious)	0 (Damaging)

Abbreviations: FIS, Functional Impact Score; GD, Grantham Difference; GVGD, Grantham Variation, Grantham Difference; PROVEAN, Protein Variation Effect Analyzer; SIFT, Sorting Intolerant From Tolerant.

[1]http://genetics.bwh.harvard.edu/pph2/. The values range from 0 to 1, with 1 being the most damaging.

[2]http://mutationassessor.org/. FIS >1.938 has medium and high significance, and they are considered disease associated.

[3]http://agvgd.hci.utah.edu/. The following classifiers, ordered from most likely to interfere with function to least likely, were used: GD ≥ [65 + tan(10) × $GV^{2.5}$] → Class C65, GD ≥ [55 + tan(10) × $GV^{2.0}$] → Class C55, Class C45, Class C35, Class C25, Class C15 and GD < [15 + tan(75) × $GV^{0.6}$] → Class C0.

[4]http://provean.jcvi.org/index.php. Values below a cutoff score of −2.5 indicate deleterious mutations.

[5]http://sift.jcvi.org/www/SIFT_enst_submit.html. The values range from 0 to 1, with 0 being the most damaging. Note that all mutations are homozygous, and to our knowledge all of them are reported for the first time in this study.

contribute to the ARCI phenotype, the discovery of the homozygous p.Ala34Pro mutation in *PNPLA1* is keeping with consanguinity noted in this family.

In one family, two heterozygous mutations in the *PNPLA1* gene were identified, one of them being the nonsense variant p.Tyr488Ter. In addition, this family had a heterozygous nucleotide substitution, c.1469C>T, affecting the last nucleotide of exon 7 at the exon 7/intron 7 border. In addition to potential amino acid substitution, p.Thr490Met, the latter base pair substitution has potential for alteration of splicing of intron 7, according to Human Splicing Finder (Aix Marseille Université, INSERM; Desmet et al., 2009). However, the allelic frequency of this variant, c.1469C>T (rs12197079), was shown to be C:0.760 and T:0.240, the phenotypic frequency of C/T being 0.348 (1000 Genomes Project Phase 3 Allele Frequencies; www.internationalgenome.org). Also, the nonsense variant p.Tyr488Ter has been shown by global sequence analysis of over 121,000 alleles to be a polymorphism with 26% frequency, the genotype being homozygous T/T in 4,519 individuals (Lek et al., 2016). Thus, we concluded that these two sequence variants, p.Tyr488Ter and c.1469C>T, are coincidental, not pathogenic findings.

Predicted consequences of the mutations at the protein level

PNPLA1 has a patatin-like domain extending from Ile16 to Thr185 that has been proposed to have an important role in lipid hydrolase activity (Grall et al., 2012). This patatin-like structure harbors a conserved catalytic center of Ser-Asp located at Ser53 and Asp172, respectively. The x-ray crystallography structure of the Pat17 *Solanum cardiophyllum* (heartleaf horsenettle weed) (Rydel et al., 2003; Wijeyesakere et al., 2014) resembling the patatin fold in PNPLA1 has shown that these residues play a pivotal role in enzymatic activity of the protein (Protein Database entry 4PK9). Moreover, the conserved motif of serine hydrolase enzymes (Gly-X-Ser-X-Gly) is also present in PNPLA1 (Gly51-Thr52-Ser53-Ala54-Gly55).

All nine missense mutations discovered thus far in PNPLA1 are located within the patatin-like domain (Figure 3). The three-dimensional model of PNPLA1 indicated that three of the mutations reported in this study (p.Thr125Asn, p.Ser19Leu, and p.Asp172Asn) are positioned at or adjacent to the active site, suggesting their involvement in aberration of catalytic activity (Figure 3). Three of these mutations (p.Ala34Pro, p.Lys141Glu, and p.Pro163Leu) are located at the surface of the protein, potentially involving protein-protein interactions (Figure 3). It should be noted that protein sequence alignment results between human PNPLA1 (PLPL1_HUMAN) and *Solanum cardiophyllum* (PAT17_SOLCD) using Clustal Omega 1.2.2 (http://www.ebi.ac.uk/tools/msa/clustalo/) indicated that the three amino acids mutated in patients (p.Thr125Asn, p.Pro163Leu, and p.Asp172Asn) were conserved between these two organisms, further strengthening the argument in support of their role in PNPLA1 structure and/or function (data available upon request).

Intra- and interfamilial phenotypic variability

Of the 26 affected individuals with homozygous *PNPLA1* mutations, 20 were available for careful clinical examination. Eight of them were male and 12 were female, ranging in age from 4 to 37 years. Examination showed considerable phenotypic heterogeneity (see Supplementary Table S1).

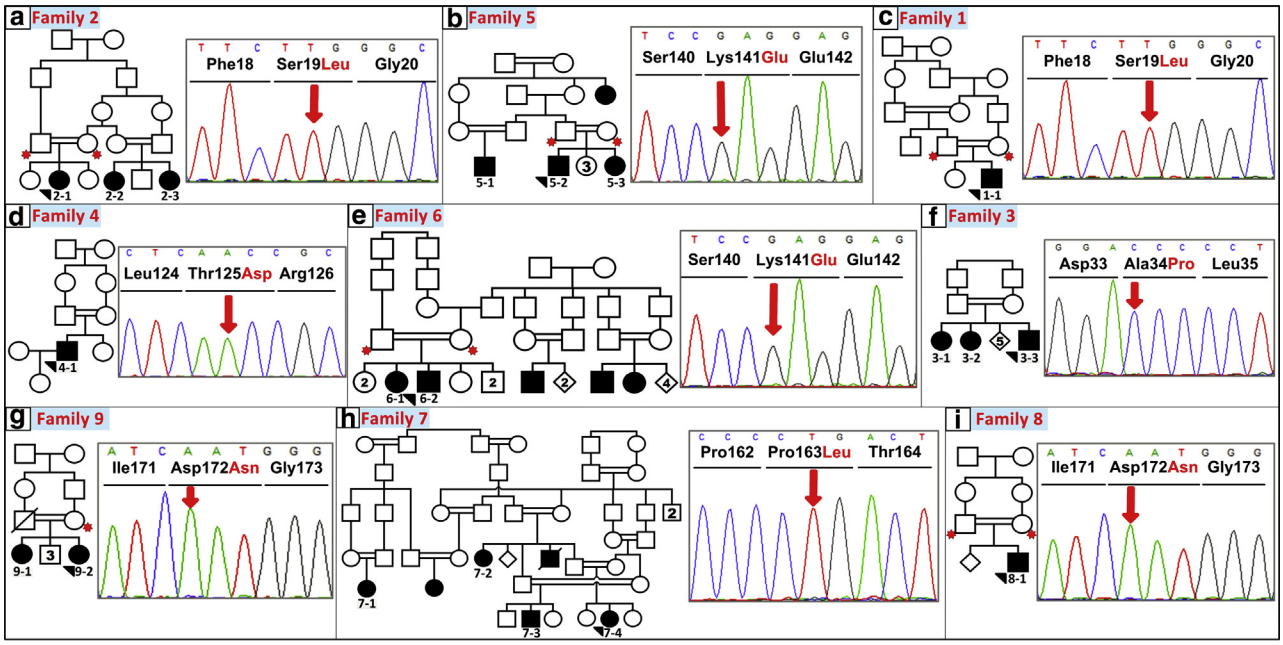

Figure 2. Family pedigrees and identification of mutations in *PNPLA1* in nine families with ichthyosis. (**a**–**i**) The probands are indicated by arrowheads, and the affected individuals tested for mutations are identified by a number (family-patient) to allow reference to Supplementary Table S1. The parents of the probands in whom the mutations were verified in the heterozygous state are indicated by red asterisks. Note the consanguinity in all families; the parents of the probands are in most cases first cousins (Table 1). The positions of the homozygous nucleotide substitutions resulting in missense mutations are indicated by red arrows.

Although all patients had generalized ichthyosis, with more severe involvement in the flexural areas (Figure 1o) as well as on the scalp, some patients had fine white scales, whereas others had large, dark, and plate-like lesions (see Figure 1e vs. 1k). All patients had facial erythroderma, anhidrosis, and acrogeric features on the backs of the hands. Nine out of 20 patients had malformed outer ears (Figure 1f and g). About half of the patients had nail dystrophy in hands and/or feet (Figure 1m). All patients had some degree of ectropion, which in most patients prevented closure of the eyes during sleep. Most, but not all, patients had palmoplantar keratoderma of varying degree, with marked hyperlinearity of the palms (Figure 1h). Subjectively, most patients complained of joint pains, and in some patients moderate joint laxity had been noted, but the relation of these symptoms to ichthyosis is not clear. Finally, for 12 of the 20 patients, there was recorded evidence of being a collodion baby at birth.

Impact of consanguinity on mutation profile

Examination of the families with affected individuals showed extensive consanguinity. For example, family 7 (Figure 2h) had 10 recorded consanguineous unions, resulting in six clinically affected individuals. All mutations identified in our study were homozygous, attesting to the impact of consanguinity (see Discussion).

DISCUSSION

The PNPLA protein family comprises nine members with lipolytic and acyltransferase activities, key elements in lipid metabolism (Lake et al., 2005; Wilson et al., 2006). There are three subfamilies, one of them consisting of PNPLA1-5. In this group, mutations in *PNPLA2* have been shown to result in neutral lipid storage disease with myopathy, and mutations in *PNPLA3* have been suggested to confer susceptibility to nonalcoholic fatty liver disease (Fischer et al., 2007; Romeo et al., 2008; Tian et al., 2010). Four mutations have been previously identified in *PNPLA1* in patients with ARCI (Ahmad et al., 2015; Fachal et al., 2014; Grall et al., 2012; Lee et al., 2016). Examination of clinical features in these patients has suggested a diagnostic clinical phenotype, the skin findings consisting of collodion membrane at birth, generalized ichthyosis including flexural areas of fine greyish-white scales, moderate erythroderma, and palmoplantar keratoderma; this entry in the *OMIM Clinical Synopsis* (#615024) has been designated as ichthyosis, congenital, autosomal recessive 10 (ARCI10). Although all patients in our study meet these clinical criteria, there is considerable variability: for example, only 12 of 20 patients were known to be born with collodion membrane. Furthermore, the severity of the ichthyosis was highly variable, and the degree of palmoplantar keratoderma was varied in presentation (Figure 1). Similar variability was noted also in members of the same family with the same mutation, implying the influence of modifying genetic and environmental factors.

PNPLA1 encodes a protein in the family with highly conserved patatin-like domain spanning the amino acid positions 16–185. All four previously identified *PNPLA1* mutations and all of the total of six distinct mutations identified in this study reside in this particular domain. Also, all six mutations identified in our study and three out of the four previously reported ones are missense mutations; only one is a nonsense mutation. These observations attest to the critical importance of the primary sequence in PNPLA1, particularly within the patatin-like domain, in maintaining the proper function of this protein. Although the precise function of PNPLA1 is currently unknown, this enzyme has a high degree of homology with PNPLA2, a major triglyceride hydrolase in

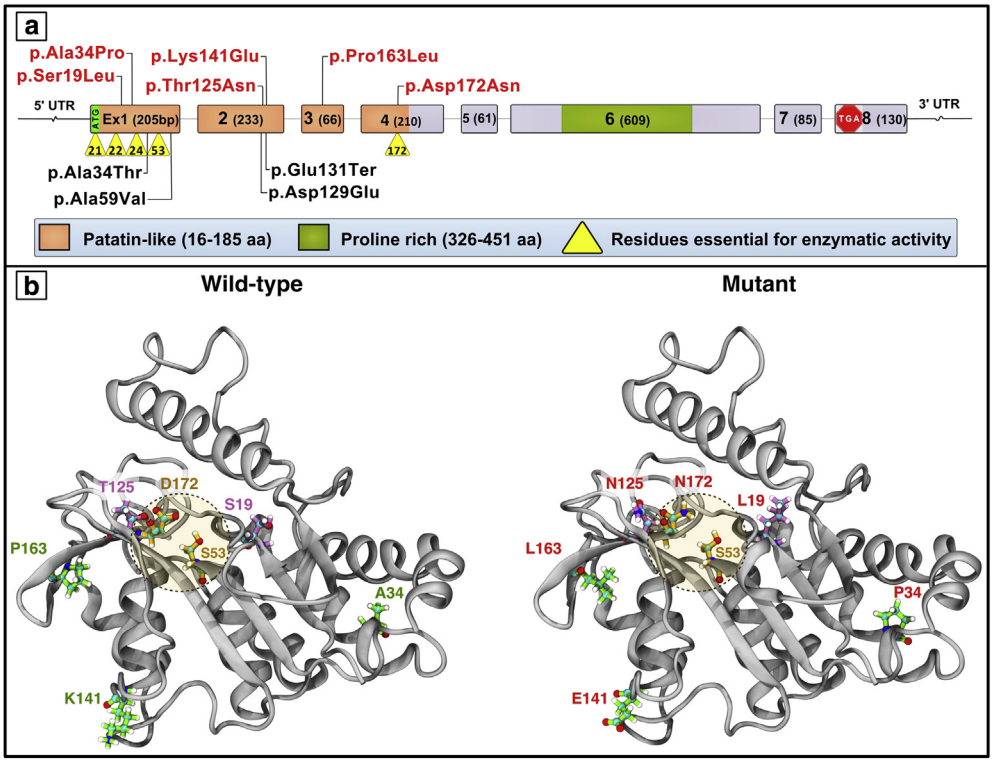

Figure 3. Gene and protein structures of *PNPLA1* and the positions of pathogenic mutations. (**a**) The *PNPLA1* gene consists of eight exons with their sizes (bp) indicated in parenthesis. (The introns are not drawn to scale). The genomic sequences encoding patatin-like and proline-rich domains are indicated. Amino acid residues essential for enzymatic activity are indicated by yellow triangles. The positions of mutations identified in this study that were, to our knowledge, previously unreported are indicated in red above the gene structure, and those previously reported are in black below. Note that all mutations reside within the gene segment encoding the patatin-like protein domain. (**b**) Structural representation of patatin-like domain of PNPLA1 (residues Ile16-Thr185) with the catalytic center adjacent to residue Ser53 being shown by dashed circle with yellow overlay. Mutations that are likely to interfere with catalytic activity are colored in pink. Mutations that are located at the protein interface are indicated in green. Oxygen, hydrogen, nitrogen, and carbon atoms are in red, white, blue, and cyan, respectively (stick-and-ball structures). Aa, amino acids; bp, base pairs; Ex, exon; TGA, stop codon; UTR, translated region.

many cell types (Grall et al., 2012). Extensive biochemical experiments with wild-type and PNPLA1-deficient keratinocytes, as well as in *Pnpla1*-knockout mice, have suggested, however, that PNPLA1 has a role in synthesis of ω-O-acyl ceramide, a sphingolipid critical for formation and maintenance of epidermal barrier (Grall et al., 2012; Grond et al., 2016; Pichery et al., 2016).

In summary, application of a gene-targeted NGS array for identification of mutations in a large cohort of Iranian patients from consanguineous families identified six mutations in *PNPLA1* that to our knowledge were previously unreported, which more than doubles the existing database on mutations in this gene. The consanguinity noted in these families clearly affects the mutations, all *PNPLA1* mutations being homozygous, a feature noted in other rare genetic skin diseases in Iranian populations, as exemplified by Kindler syndrome, epidermolysis bullosa simplex, and hyaline fibromatosis syndrome (Vahidnezhad et al., 2016; Youssefian et al., 2015, 2016). Examination of the patients showed considerable intra- and interfamilial heterogeneity in clinical presentation. Identification of specific mutations in this population with a high degree of consanguinity will help identify heterozygous carriers in extended families with a history of ARCI and will facilitate counseling toward eradication of heritable skin diseases, including ARCI, through genetic counseling, prenatal testing, and preimplantation genetic diagnosis.

MATERIALS AND METHODS

Patient data

This study was approved by the institutional review board of the Pasteur Institute of Iran, and all subjects and parents of underaged patients gave written informed consent to participate in research and to publish their images. In this study, 92 extended families affected by nonsyndromic and syndromic forms of ichthyosis, diagnosed in various medical centers in Iran, were evaluated. The families were personally examined by dermatologists (MRB, SS, PM) and by medical geneticists (LY and HV), who are authors, and the diagnostic clinical features and demographic data were carefully recorded. Criteria for inclusion were clinical presentation of ichthyosis supported in some of the patients by histopathology (Figure 1).

NGS and data analysis

DNA was extracted from peripheral blood samples by a kit (QIAamp Blood Maxi Kit; Qiagen, Valencia, CA) or by salting-out method. DNA concentration was measured using a Qubit 2.0 fluorometer (Life Technologies, Carlsbad, CA). Target enrichment was performed using the TruSeq Custom Amplicon kit (Illumina, San Diego). DesignStudio (Illumina) was used for library design. All coding exons, at least 20 bp of the intron at each intron-exon boundary, and up to 50 bp of 3′-untranslated regions were targeted. The designed library contained 38 genes (*ABCA12*, *ABHD5*, *AGPS*, *ALDH3A2*, *ALOX12B*, *ALOXE3*, *AP1S1*, *ARSE*, *CERS3*, *CLDN1*, *CYP4F22*, *EBP*, *ELOVL4*, *GJB2*, *GJB3*, *GJB4*, *GJB6*, *KRT1*, *KRT10*, *KRT2*, *KRT9*, *LIPN*, *LOR*, *NIPAL4*, *PEX7*, *PHYH*, *PNPLA1*, *PNPLA2*, *POMP*, *SLC27A4*, *SNAP29*, *SPINK5*, *ST14*, *STS*, *TGM1*, *TGM5*, *VPS33B*, and *ZMPSTE24*) divided into 351 targets covered by 558 amplicon probes, which were designed to cover 99% of targeted bases. A total of 93.2% of the reads were aligned to the human genome, with the mean coverage of the target region being 493×. In addition, only 0.4% of bases of the target region were not covered by any sequence read, indicating that 99.6% of all target region bases were sequenced at least once. Genomic DNA from 92 probands, each

representative of a distinct extended family, and two Illumina controls were multiplexed using dual indexing with 12 primary indexes and eight secondary indexes. Dual-indexed samples were normalized to be equimolar and were pooled together following manufacturer's recommendations. The pool was sequenced on a single MiSeq flow-cell (Illumina). Reads were paired end at 2 × 225 nucleotides with dual indexes, and a total of 8.49 giga-base pairs were generated. All samples passed quality control. Reads were aligned to the human genome version hg19 (Lander et al., 2001) using the BaseSpace MiSeq Reporterworkflow version 2.4 TruSeq Amplicon App by Illumina. This software implements the banded Smith-Waterman algorithm in the targeted regions (specified in the Illumina manifest file). Picard Tools ReorderSam was used to properly format each alignment file (https://broadinstitute.github.io/picard/). Genome Analysis Took Kit tools RealignerTargertCreator, IndelRealigner, BaseRecalibrator, and PrintReads were used to preprocess the alignments, utilizing local alignments and base quality score distributions to optimize alignment accuracy. Variants were called with GATK HaplotypeCaller.

PCR and Sanger sequencing

PCR was performed using *Taq* polymerase (Qiagen) according to the manufacturer's instructions. Amplification of the *PNPLA1* gene was performed with eight pairs of newly designed primers (sequences available upon request), spanning all eight exons and the flanking intronic sequences. The PCR products were bidirectionally sequenced using an automated sequencer (3730; Applied Biosystems, Foster City, CA). The mutation positions are reported in reference to NM_001145717 (cDNA) and NP_001139189 (protein).

Protein modeling

Three-dimensional structures were modeled using SWISS-MODEL (available at http://swissmodel.expasy.org/). Hydrogen atoms were added by Reduce 3.23 (Word et al., 1999). Mutant and wild-type structures were generated using the psfgen plugin (version 1.6.4) of the Visual Molecular Dynamics (Humphrey et al., 1996). The Nanoscale Molecular Dynamics software package was used for energy minimization by conjugate gradient algorithm for 10,000 steps to remove bad contacts (Phillips et al., 2005). Molecular graphics were created by VMD 1.9.2.

CONFLICT OF INTEREST

The authors state no conflict of interest.

ACKNOWLEDGMENTS

We thank the patients and their families for participation and Kaveh Khademhossein, Zahrasadat Ghoreishi, Maryam Karami Bozanjani, and Sina Shamsi for patient referral. Carol Kelly assisted in manuscript preparation.

SUPPLEMENTARY MATERIAL

Supplementary material is linked to the online version of the paper at www.jidonline.org, and at http://dx.doi.org/10.1016/j.jid.2016.11.012.

REFERENCES

Ahmad F, Ansar M, Mehmood S, Izoduwa A, Lee K, Nasir A, et al. A novel missense variant in the PNPLA1 gene underlies congenital ichthyosis in three consanguineous families. J Eur Acad Dermatol Venereol 2015;30:e210–3.

Alef T, Torres S, Hausser I, Metze D, Tursen U, Lestringant GG, et al. Ichthyosis, follicular atrophoderma, and hypotrichosis caused by mutations in ST14 is associated with impaired profilaggrin processing. J Invest Dermatol 2009;129:862–9.

Baden HP, Digiovanna JJ. Ichthyosiform dermatoses. In: Rimoin DL, Korf B, editors. Emery and Rimoin's principle and practice of medical genetics. Philadelphia, PA: Academic Press; 2013. p. 1–26.

Basel-Vanagaite L, Attia R, Ishida-Yamamoto A, Rainshtein L, Ben Amitai D, Lurie R, et al. Autosomal recessive ichthyosis with hypotrichosis caused by a mutation in ST14, encoding type II transmembrane serine protease matriptase. Am J Hum Genet 2007;80:467–77.

Desmet FO, Hamroun D, Lalande M, Collod-Beroud G, Claustres M, Beroud C. Human Splicing Finder: an online bioinformatics tool to predict splicing signals. Nucleic Acid Res 2009;37:e67.

Fachal L, Rodriguez-Pazos L, Ginarte M, Carracedo A, Toribio J, Vega A. Identification of a novel PNPLA1 mutation in a Spanish family with autosomal recessive congenital ichthyosis. Br J Dermatol 2014;170:980–2.

Fischer J, Lefevre C, Morava E, Mussini JM, Laforet P, Negre-Salvayre A, et al. The gene encoding adipose triglyceride lipase (PNPLA2) is mutated in neutral lipid storage disease with myopathy. Nat Genet 2007;39:28–30.

Grall A, Guaguere E, Planchais S, Grond S, Bourrat E, Hausser I, et al. PNPLA1 mutations cause autosomal recessive congenital ichthyosis in golden retriever dogs and humans. Nat Genet 2012;44:140–7.

Grond S, Eichmann T, Dubrac S, Kolb D, Schmuth M, Fischer J, et al. PNPLA1 deficiency in mice and humans leads to a defect in the synthesis of ω-O-acylceramides [e-pub ahead of print]. J Invest Dermatol 2016; http://dx.doi.org/10.1016/j.jid.2016.08.036 (accessed December 19, 2016).

Humphrey W, Dalke A, Schulten K. VMD: visual molecular dynamics. J Mol Graph 1996;14:33–8, 27–8.

Lake AC, Sun Y, Li JL, Kim JE, Johnson JW, Li D, et al. Expression, regulation, and triglyceride hydrolase activity of Adiponutrin family members. J Lipid Res 2005;46:2477–87.

Lander ES, Linton LM, Birren B, Nusbaum C, Zody MC, Baldwin J, et al. Initial sequencing and analysis of the human genome. Nature 2001;409:860–921.

Lee E, Rahman OU, Khan MT, Wadood A, Naeem M, Kang C, et al. Whole exome analysis reveals a novel missense PNPLA1 variant that causes autosomal recessive congenital ichthyosis in a Pakistani family. J Dermatol Sci 2016;82:46–8.

Lek M, Karczewski KJ, Minikel EV, Samocha KE, Banks E, Fennell T, et al. Analysis of protein-coding genetic variation in 60,706 humans. Nature 2016;536:285–91.

Phillips JC, Braun R, Wang W, Gumbart J, Tajkhorshid E, Villa E, et al. Scalable molecular dynamics with NAMD. J Comput Chem 2005;26:1781–802.

Pichery M, Huchenq A, Sandhoff R, Roy M, Severino-Freire M, Zaafouri S, et al. PNPLA1 defects in patients with ichthyosis and KO mice unveil PNPLA1 irreplaceable function in epidermal omega-acylceramide synthesis and skin permeability barrier. J Invest Dermatol 2016;136:S180.

Richard G, Bale SJ. Autosomal recessive congenital ichthyosis. In: Pagon R, Adam MP, Ardinger HH, Wallace SE, Amemiya A, Bean LJH, et al., editors. Gene reviews. Seattle, WA: University of Washington; 2014. p. 1993–2016.

Romeo S, Kozlitina J, Xing C, Pertsemlidis A, Cox D, Pennacchio LA, et al. Genetic variation in PNPLA3 confers susceptibility to nonalcoholic fatty liver disease. Nat Genet 2008;40:1461–5.

Rydel TJ, Williams JM, Krieger E, Moshiri F, Stallings WC, Brown SM, et al. The crystal structure, mutagenesis, and activity studies reveal that patatin is a lipid acyl hydrolase with a Ser-Asp catalytic dyad. Biochemistry (Mosc) 2003;42:6696–708.

Schmuth M, Martinz V, Janecke AR, Fauth C, Schossig A, Zschocke J, et al. Inherited ichthyoses/generalized Mendelian disorders of cornification. Eur J Hum Genet 2013;21:123–33.

South AP, Li Q, Uitto J. Next-generation sequencing for mutation detection in heritable skin diseases: the paradigm of pseudoxanthoma elasticum. J Invest Dermatol 2015;135:937–40.

Takeichi T, Nanda A, Liu L, Salam A, Campbell P, Fong K, et al. Impact of next generation sequencing on diagnostics in a genetic skin disease clinic. Exp Dermatol 2013;22:825–31.

Tian C, Stokowski RP, Kershenobich D, Ballinger DG, Hinds DA. Variant in PNPLA3 is associated with alcoholic liver disease. Nat Genet 2010;42:21–3.

Vahidnezhad H, Youssefian L, Saeidian AH, Mozafari N, Barzegar MR, Sotoudeh S, et al. KRT5 and KRT14 mutations in epidermolysis bullosa simplex with phenotypic heterogeneity, and evidence of semi-dominant inheritance in a multiplex family. J Invest Dermatol 2016;136:1897–901.

Wijeyesakere SJ, Richardson RJ, Stuckey JA. Crystal structure of patatin-17 in complex with aged and non-aged organophosphorus compounds. PLoS One 2014;9:e108245.

Wilson PA, Gardner SD, Lambie NM, Commans SA, Crowther DJ. Characterization of the human patatin-like phospholipase family. J Lipid Res 2006;47:1940–9.

Word JM, Lovell SC, Richardson JS, Richardson DC. Asparagine and glutamine: using hydrogen atom contacts in the choice of side-chain amide orientation. J Mol Biol 1999;285:1735–47.

Youssefian L, Vahidnezhad H, Aghighi Y, Ziaee V, Zeinali S, Abiri M, et al. Hyaline fibromatosis syndrome: A novel mutation and recurrent founder mutation in the CMG2/ANTXR2 gene [e-pub ahead of print]. Acta Derm Venereol 2016; http://dx.doi.org/10.2340/00015555-2459 (accessed December 19, 2016).

Youssefian L, Vahidnezhad H, Barzegar M, Li Q, Sotoudeh S, Yazdanfar A, et al. The Kindler syndrome: a spectrum of FERMT1 mutations in Iranian families. J Invest Dermatol 2015;135:1447–50.